Plastic buckling of short cylinders under transverse shearing loads

Y.Kawamoto & T.Yuhara
Nagasaki R&D Center, Mitsubishi Heavy Industries Ltd, Japan
M.Tashimo
Kobe Shipyard & Engine Works, Mitsubishi Heavy Industries Ltd, Japan
A.Sakurai & H.Nakamura
Central Research Institute of Electric Power Industry, Chiba, Japan

1 INTRODUCTION

Nuclear power plant components are greatly demanded to withstand against strong earthquake in Japan.Initially the feasibility studies for a pool-type fast breeder reactor in Japan were performed from 1981 to 1983 by Central Research Institute of Electric Power Industry (CRIEPI) in cooperation with some nuclear plant fabricators. Continuously, in order to reduce the construction cost and improve the reliability of the plant, the advanced studies have been carried out from 1984 to 1986 by CRIEPI, Mitsubishi Heavy Industries, Ltd. (MHI), Hitachi Ltd. and Toshiba Corp. In a part of these studies, four buckling test programs have been performed to make the buckling strength of a pool-type fast breeder reactor clear (Nakamura 1987, Kokubo 1987, Murakami 1987). In this paper, a buckling test program for plastic shear buckling of short cylinders conducted by MHI is reported.

If a pool-type fast breeder reactor is subjected to severe seismic loads, the cylindrical shell of a main vessel might fail by shear buckling due to horizontal inertia forces. Therefore, we investigate the plastic shear buckling of short cylinders. The buckling of cylinders subjected to transverse shearing loads has been studied by some researchers. On elastic shear buckling, Schröder (1972) and Yamaki, et al. (1979) individually obtained an approximate solution using Donnell's shell equations in conjunction with Galerkin's method. Lundquist (1935) carried out many elastic shear buckling tests of moderately long duralumin cylinders, and Yamaki, et al. (1979) tested some short cylinders which were made from polyester film. On plastic shear buckling in the actual design problem, a few relevant tests have been found in the open literature. Galletly, et al. (1985) recently presented a paper on this subject. In their study, 14 small steel models were tested under transverse shearing loads. They, however, didn't describe the post-buckling behavior of the model.

We consider the static analogue on buckling behavior under seismic loads and conduct 4 static buckling tests using 1/20 scale cylindrical models of a main vessel. We obtain not only the buckling strength but also the post-buckling behavior under repeated shearing loads. In addition, we carry out the non-linear numerical analysis to simulate plastic shear buckling behavior and get a good agreement with experimental results. We study further parametric calculations to clarify the effect of initial imperfection on plastic shear buckling.

2 BUCKLING TESTS

2.1 Models and test setup

The geometric and material properties for the 4 models are given in Table 1. The models, having a nominal diameter of 800 mm and a nominal length of 400 mm, are approximately 1/20 the size of the actual cylindrical shell of the main vessel. The shell thickness is varied from 1.2 mm to 3.0 mm to examine the effect of radius-to-thickness ratio (R/t) on shear buckling. And two different materials, stainless steel and mild steel, are used for fabricating the models to investigate the effect of material characteristic. Each model is fabricated by rolling a steel plate into a cylindrical form and welding together the rolled plate edges longitudinally. Flanges are welded onto the ends of the model. No stress relief is carried out.

The buckling tests are performed on a 125ton capacity structural test rig owned by MHI. The test setup is shown in Fig.1. The transverse shearing load is applied at a point 480 mm apart from the base of the vertically cantilevered model. Thus, the bending stress-to-shear stress ratio (σ_b/τ) at the base of the model becomes approximately 1.2, and seems to be nearly equal to that of the actual vessel under seismic loads.

2.2 Test results

Before the test, each model is carefully measured its dimensions and initial imperfections. Each model is satisfactorily fabricated according to its nominal dimensions. An example of the measured initial imperfections is shown in Fig.2. The maximum amplitude of initial radial imperfection in each model is less than 1 mm.

Applying the transverse shearing load to each model, the shearing deformation at first appears at the side shell wall and then the load immediately reaches the maximum load. Therefore,we regard the maximum load as the buckling load. With further application of the shearing load, the shell wall deformation progressively increases until the entire wall is buckled with diagonal buckles. As an example, the photograph of the buckles in model SUS-2.0 is shown in Photo.1. The transverse shearing load is reversed, and the shell wall becomes similarly buckled in the opposite direction. And, the model is loaded repeatedly to determine the restoring force characteristic, which is required in analyzing the vessel's dynamic response against earthquake. Typical transverse shearing load versus horizontal displacement curves for the model are shown in Fig.3. Obviously, the model exhibits relatively stable behavior even after the buckling under repeated load, and thus has a capacity to absorb considerably large energy input. The shear buckling tests enable us to imagine the buckling behavior of a main vessel under extreme seismic loads.

A summary of the buckling test results is given in Table 2. And the relation between the buckling strength and the radius-to-thickness ratio (R/t) is indicated in Fig.4. The buckling strength normalized by the shear yielding load is expressed. The shear yielding load (Q_o) means the load at which the maximum shear stress in each model reaches the shear yield stress. Q_o is expressed as a following equation.

(1) $Q_o = \pi Rt \cdot \tau_o$

where τ_o is the shear yield stress as taken $\sigma_o/\sqrt{3}$ herein. The solid line in Fig.4 shows the predicted buckling load by a following quadratic

interaction formula using the typical material properties.

(2) $$\frac{1}{Q_{max}^2} = \frac{1}{Q_o^2} + \frac{1}{Q_{cr}^{e2}}$$

where Q_o is the shear yielding load and Q_{cr}^e is the elastic shear buckling load estimated by Yamaki's method (1979). The predicted values give a good estimation of the buckling load in the limited range of geometries investigated.

As given in Table 1, 3mm-thick models, SUS-3.0 and MS-3.0, are made from two different materials to examine the effect of material characteristic on plastic shear buckling. No significant difference in the normalized buckling loads (Q_{max}/Q_o) is recognized. But the rate of decrease of load after reaching the maximum load for model SUS-3.0 is lower than that for model MS-3.0. As the stainless steel has considerable strain hardening, the stainless steel model seems to have relatively higher post-buckling strength than the mild steel model.

3 NUMERICAL ANALYSIS

3.1 Comparison with the test result

Non-linear finite element analysis is carried out to simulate the buckling behavior using STAGSC-1 code. The deflection reproduced from the measured initial imperfection by applying Fourier expansions are formerly introduced in a finite-element model. As an example, the comparison between the STAGSC-1's solution and the experimental result for model SUS-2.0 is shown in Fig.5. The difference between the maximum loads is less than 3%. The reliable predicted maximum load can be obtained by using STAGSC-1 code with some techniques. But there are some difficulties in obtaining the post-buckling behavior by numerical analysis in the present state. The calculated buckling deformation is shown Fig.6, which is overlapped the finite element model. Application of force to the model in the direction indicated by the arrow produces diagonal buckles in the side shell wall due to shearing, in very much the same manner as in the buckling test.

3.2 Parametric study

In order to examine the effect of initial imperfection on plastic shear buckling, several non-linear calculations are performed using STAGSC-1 code which differ in the maximum amplitude of initial deflection. The nondimensional load-displacement curves are indicated in Fig.7. In the series of calculations, the same mode of initial deflection is introduced into the model as the elastic buckling mode which is estimated by Yamaki's method. And the geometric parameters and the material properties are applied the following values to simulate the actual conditions of the main vessel of a pool-type reactor.

(3) $R/t = 200$, $L/R = 1.0$, $H/R = 1.2$

(4) $E = 17{,}600\ kg/mm^2$, $\sigma_o = 15.7\ kg/mm^2$.

As a summary of numerical results, the relation between the buckling load and the amplitude of initial imperfection is indicated in Fig.8. The effect of initial imperfection on plastic shear buckling is remarkably smaller than that on elastic axial buckling.

The reduction of buckling strength at $W_{max}/t=0.5$ is less than 10% on plastic shear buckling.

4 CONCLUSIONS

The conclusions made from the present investigation on plastic shear buckling are as follows:

1. The plastic shear buckling strength of short cylinders is obtained experimentally. The buckling load of the main vessel of a pool-type FBR is estimated to be approximately 85% of the shear yielding load.
2. The post-buckling behavior on plastic shear buckling is relatively stable under repeated loads. The vessel is estimated to have a considerably large capacity to absorb seismic energy input.
3. The buckling load can be estimated by the non-linear analysis using STAGSC-1 code with a sufficient accuracy.
4. The effect of initial imperfection is remarkably small. The reduction of buckling strength at $W_{max}/t=0.5$ is at most 10%.

REFERENCES

Nakamura, H. et al. 1987. Plastic buckling of short cylinders with axial temperature distribution under transverse shearing loads. to be presented for SMiRT-9.

Kokubo, K. et al. 1987. Buckling behaviors of short cylindrical shells under dynamic loads. to be presented for SMiRT-9.

Murakami, T. et al. 1987. Buckling strength of elliptical heads with core support structure under vertical and horizontal loads. to be presented for SMiRT-9.

Galletly, G.D. & J.Blachut. 1985. Plastic buckling of short vertical cylindrical shells subjected to horizontal edge shear loads. J. Pressure Vessel Technol. 107 : 101-106.

Schröder, P. 1972. Über die Stabilität der Querkraftbelasteten dünnwandigen Kreiszylinderschale. ZAMM. 52 : T145-T148.

Lundquist, E.E. 1935. Strength tests of thin-walled duralumin cylinders in combined transverse shear and bending. NACA TN-523.

Yamaki, N., K.Naito & E.Sato. 1979. Buckling of Circular cylindrical shells under combined action of a transverse edge load and hydrostatic pressure. Proc. int. conf. thin-walled struct.

Table 1. Geometric and material properties for the models.

Model	Material		Dimensions			Geometric Parameter		
	σ_o (kg/mm^2)	E (kg/mm^2)	D (mm)	L (mm)	t (mm)	L/R	R/t	H/R
SUS-3.0	24.9	19,400	800	400	3.0	1.0	133	1.2
SUS-2.0	26.1	19,500	800	400	2.0	1.0	200	1.2
SUS-1.2	24.1	19,400	800	400	1.2	1.0	333	1.2
MS-3.0	29.2	20,800	800	400	3.0	1.0	133	1.2

"SUS" and "MS" mean respectively stainless steel and mild steel.

Table 2. Test results.

Model	Qmax (ton)	τ_{max} (kg/mm^2)	Qmax/Qo
SUS-3.0	56.0	14.8	1.03
SUS-2.0	31.3	12.4	0.82
SUS-1.2	12.0	7.9	0.57
MS-3.0	64.8	17.1	1.02

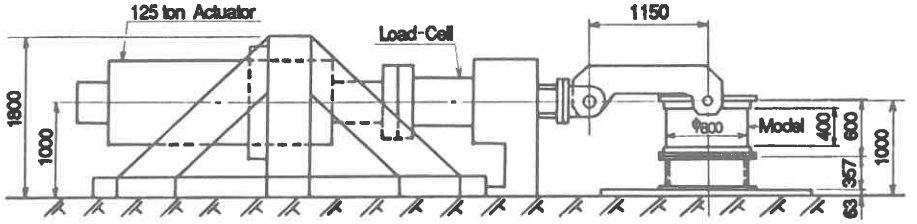

Fig.1 Test setup

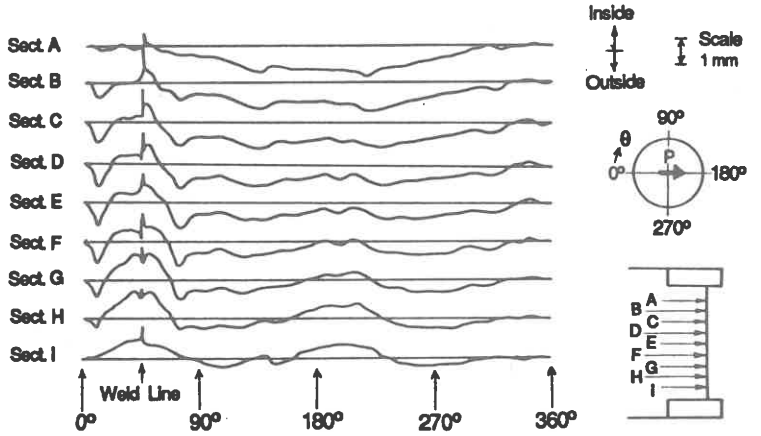

Fig.2 The circumferential distributions of initial radial imperfections for model SUS-2.0

Photo.1 Buckles in model SUS-2.0

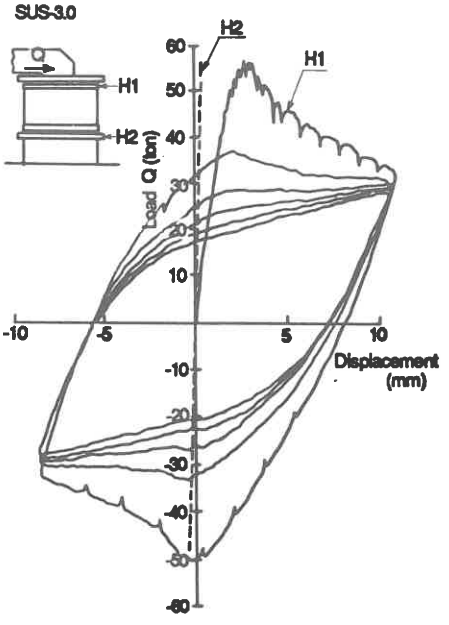

Fig.3 Load-displacement curve of model SUS-3.0

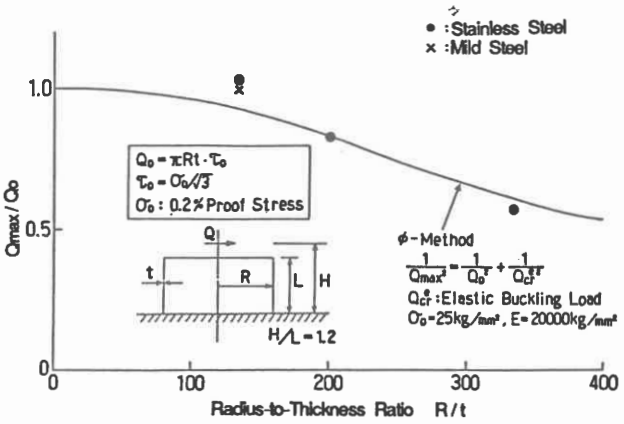

Fig.4 Test results (buckling load v.s. radius-to-thickness ratio)

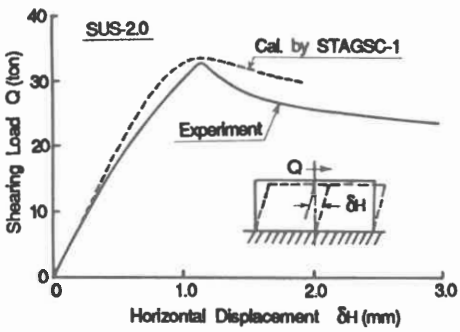

Fig.5 Comparison between numerical and experimental results

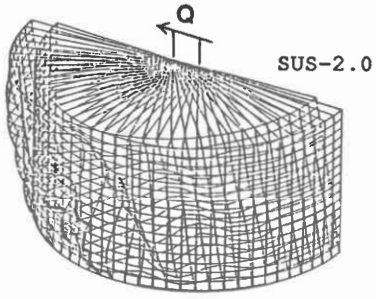

Fig.6 Shear buckling deformation by numerical analysis (using STAGSC-1)

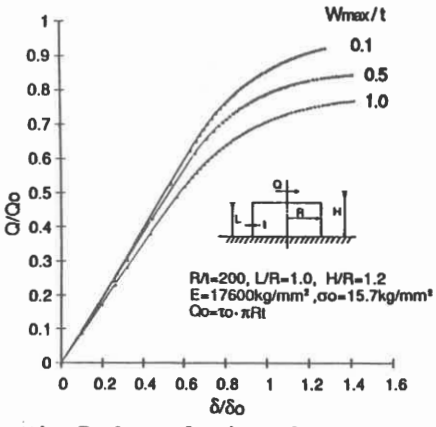

Fig.7 The relations between shearing loads and horizontal displacements.

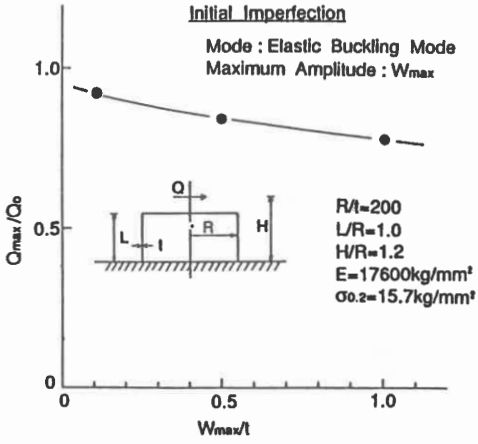

Fig.8 The effect of initial imperfection on plastic shear buckling.